GAMMA-RAY ATTENUATION FACTORS FOR ANGULAR CORRELATION AND ANGULAR DISTRIBUTION MEASUREMENTS

by

JOSEPH ALFRED MANSFIELD

A THESIS

submitted to

OREGON STATE UNIVERSITY

in partial fulfillment of
the requirements for the
degree of

MASTER OF SCIENCE

June 1962

APPROVED:

Redacted for Privacy

Associate Professor of Physics

In Charge of Major

Redacted for Privacy

Chairman of the Physics Department

Redacted for Privacy

Chairman of School Graduate Committee

Redacted for Privacy

Dean of Graduate School

Date thesis is presented April 11, 1962

Typed by Elaine Anderson

ACKNOWLEDGMENTS

The writer wishes to express appreciation to his major professor, Dr. Larry Schecter, for, of course, those things major professors are usually appreciated for, but in particular, for an opportunity to observe a professional experimentalist. Many thanks also to Mr. Lamar Coleman for his frequent and helpful discussions related to the experiment, and to Dr. E. A. Yunker for his assistance and encouragement throughout the project.

Grateful acknowledgment is further due Mr. Jack McKenzie of the Oregon State University cyclotron staff for the production of sources, Messrs. Chuck Mansfield and Cary Haig whose assistance was indeed timely, and to one of those typists, Elaine Anderson, who prints that which is intended in spite of the original.

TABLE OF CONTENTS

	Page
INTRODUCTION	1
EXPERIMENTAL ARRANGEMENT	9
RESULTS	15
Bibliography	17
APPENDIX	18

LIST OF TABLES

		Page
Table I	Elements from which energy peaks were gained.	13
Table II	Experimental values of J_n/J_o	15
Table III	Uncertainties of J_n/J_o	20

LIST OF FIGURES

Figure 1.	Geometry of the detectors	3
Figure 2.	Block diagram of the experimental apparatus.	10
Figure 3.	Typical graph of the integrand of J_n versus angle β	12
Figure 4.	Pulse height spectrum	12
Figure 5.	Attenuation factors versus energy . .	16

GAMMA-RAY ATTENUATION FACTORS FOR ANGULAR CORRELATION AND ANGULAR DISTRIBUTION MEASUREMENTS

INTRODUCTION

The experiment to be described is intimately associated with both angular distribution and angular correlation experiments and it will be useful to discuss distribution and correlation functions. In many nuclear phenomena, it is of interest to determine the angular distribution of particles emitted by a source, or the directional correlation between pairs of particles emitted by a source. In nuclear theory, the distribution and correlation functions which describe these effects can be calculated.

It is often convenient to represent such functions, called $W(\Theta)$, in terms of Legendre polynomial expansions (4, p. 610)

$$W(\Theta) = \sum_{n=0}^{m} \alpha_n P_n (\cos \Theta) \qquad (1)$$

where, for angular distribution functions, Θ is the angle between a particular direction in space and the propagation direction of the particles under consideration, and for angular correlation functions is the angle between propagation directions of the coincident particles under consideration. $W(\Theta)$ is the probability per unit solid angle of the emission at angle Θ of a particle of one

particular energy.

This form of $W(\Theta)$ is not, however, conducive to the direct experimental determination of the constants α_n since that would require a detector having dimension in only one direction. Therefore $W(\Theta)$ is altered so as to fit a physically realizable situation; that is, a mathematical process is imposed upon $W(\Theta)$ such that the result will correspond to a quantity that is measurable, and further, this result contains the various α_n, thus enabling their experimental determination. This operation on $W(\Theta)$, discussed in more detail below, results in a function $\overline{W(\Theta)}$ differing from $W(\Theta)$ in that each term is multiplied by a quantity Q; that is,

$$\overline{W(\Theta)} = \sum_{n=o}^{m} Q_n \alpha_n P_n (\cos \Theta). \qquad (2)$$

The significance of Q_n will present itself in the mathematical development of $\overline{W(\Theta)}$.

Consider first a single cylindrical region of space, such as region 2 Figure 1, symmetrically located about the angle Θ and subtending a total solid angle w_2 with respect to the origin together with a source of particles located at the origin. Let $\epsilon_2(\delta, \phi)$ be the fraction of these particles entering region 2 at angles δ and ϕ that are detected by the region so that the total number detected per second is

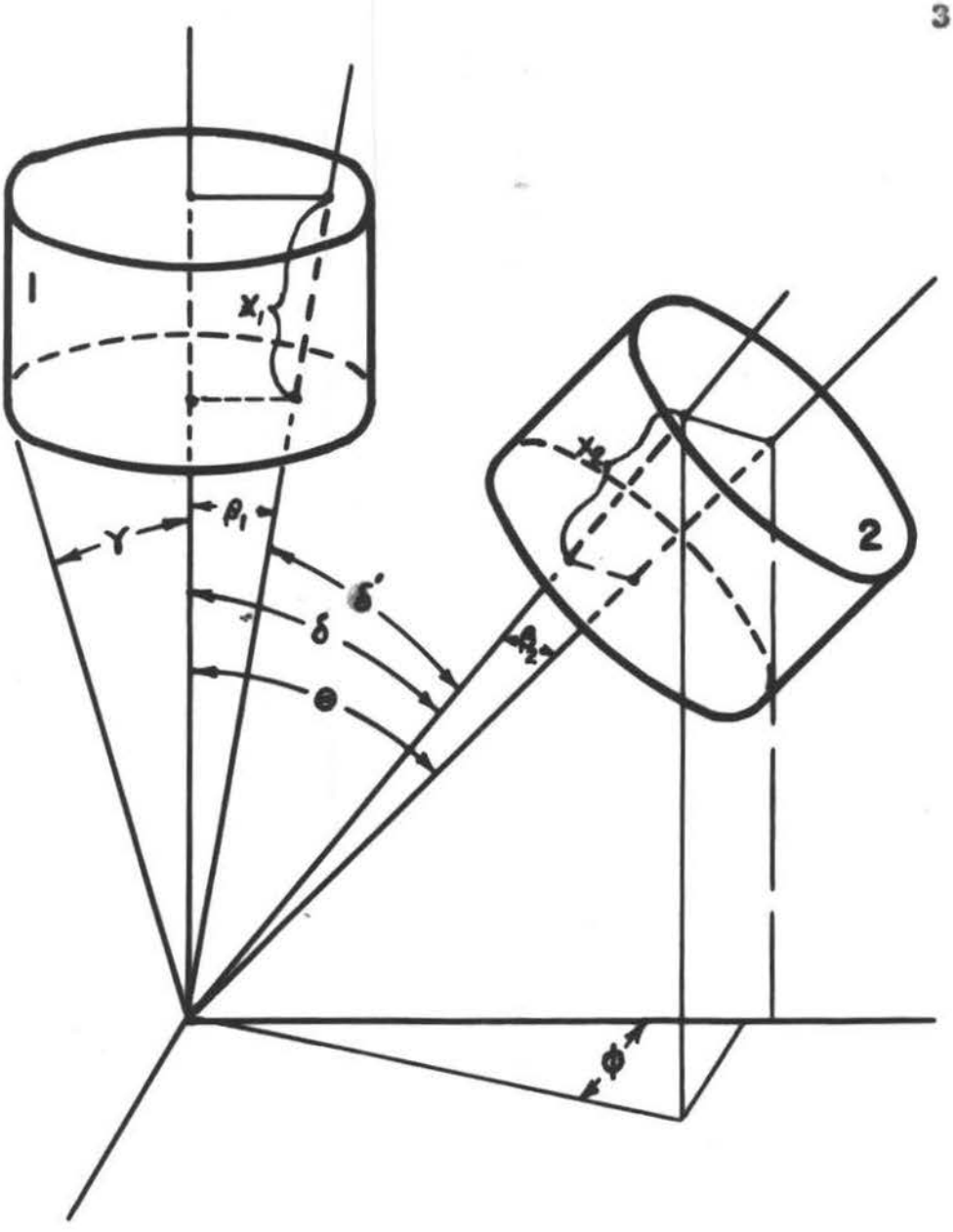

Figure 1. Geometry of the detectors.

$$C_2(\Theta) = K_2 \int W(\delta)\, \epsilon_2(\delta, \phi)\, dw_2 = K_2\, \overline{W(\Theta)} \int \epsilon_2(\delta, \phi)\, dw_2. \qquad (3)$$

Particularizing the property ϵ_2 of region 2 to a form $(1 - e^{-\tau x_2(\delta, \phi)})$, corresponding to the fraction of gamma rays of a particular energy absorbed by actual scintillation crystals, where τ is the absorption coefficient of the region for this energy, and changing variables results in

$$\int \epsilon_2(\delta, \phi)\, dw_2 = \int_0^{\gamma} \int_{-\phi}^{\phi} (1 - e^{\tau x(\beta)}) \sin\beta\, d\beta\, d\phi$$

where β is the angle between the axis of the region and the direction of the gamma rays. It is important to note that this integral is a function only of the properties and dimensions of the crystal and specifically not a function of Θ. This being so, equation (1) indicates that $C_2(\Theta)$ is different from $\overline{W(\Theta)}$ only by a constant multiplier. Thus an experimental counting rate would be proportional to $\overline{W(\Theta)}$ which, it will be seen, explicitly contains $W(\Theta)$.

It is now necessary to evaluate $\overline{W(\Theta)}$. From (3)

$$\overline{W(\Theta)} = \frac{\int_0^{\gamma} W(\delta)\, (1 - e^{-\tau x(\beta)}) \sin\beta\, d\beta}{\int_0^{\gamma} (1 - e^{-\tau x(\beta)}) \sin\beta\, d\beta}$$

which becomes upon inserting (1)

$$\overline{W(\Theta)} = \frac{\int_0^{\gamma} \sum_{n=0}^{m} \alpha_n P_n(\cos\delta)\,(1 - e^{-\tau x(\beta)})\,\sin\beta d\beta}{\int_0^{\gamma}(1 - e^{-\tau x(\beta)})\,\sin\beta d\beta}.$$

Integrals of the form

$$I_n = \alpha_n \int_0^{\gamma} P_n(\cos\delta)\,(1 - e^{-\tau x(\beta)})\,\sin\beta d\beta$$

may be simplified by substitution of the Legendre polynomial addition theorem (2, p. 109)

$$P_n(\cos\delta) = P_n(\cos\Theta)\,P_n(\cos\beta).$$

$\overline{W(\Theta)}$ then becomes

$$\overline{W(\Theta)} = \sum_{n=0}^{m} J_n/J_o \quad \alpha_n P_n(\cos\Theta), \quad (n = 0,2,4)$$

where

$$J_n = \int_0^{\gamma} P_n(\cos\beta)\,(1 - e^{-\tau x(\beta)})\,\sin\beta d\beta. \qquad (4)$$

The Q_n of equation (2) for angular distribution experiments then are

$$Q_n = J_n/J_o.$$

Thus, a knowledge of Q_n makes it possible to connect an experimentally determined distribution using finite sized detectors with the idealized distribution function. It is usually the latter which is associated with physical theory.

An angular correlation function $W(\Theta)$ may in a like manner be altered to give a function $\overline{W(\Theta)}$ proportional to the coincident counting rate (4, p. 611) for two gamma-rays defined as

$$\overline{W(\Theta)} = \frac{\int W(\delta')(1-e^{-\gamma_1(E_1)x_1(\beta_1)})(1-e^{-\gamma_2(E_2)x_2(\beta_2)})dw_1dw_2}{\int (1-e^{-\gamma_1(E_1)x_1(\beta_1)})(1-e^{-\gamma_2(E_2)x_2(\beta_2)})dw_1dw_2}$$

where γ_1 and γ_2 are the absorption coefficients of regions 1 and 2, E_1 and E_2 are the energies of the gamma-rays considered in region 1 and 2 respectively, and the other parameters are indicated in Figure 1. The Q_n, evaluated analogously, becomes

$$Q_n = J_n(1)\ J_n(2)/J_o(1)\ J_o(2)$$

where $J_n(1)$ refers to detector 1, so that

$$J_n(1) = \int_0^{\gamma_1} P_n(\cos\beta_1)(1-e^{-\gamma_1(E_1)x_1(\beta_1)})\sin\beta_1 d\beta_1$$

and similarly for $J_n(2)$, $J_o(1)$, and $J_o(2)$. For identical detectors at a common source distance and energies such that $\gamma_1 \approx \gamma_2$,

$$Q_n = (J_n/J_o)^2.$$

Consider a cylindrical scintillation crystal, optically coupled to a photomultiplier tube which in turn is coupled to an electrical pulse counting device, in the vicinity of a gamma-ray emitting point source such that the axis of the cylinder extends through the source and the half angle subtended by the front face of the region is γ (Figure 1). In particular, consider only those gamma-rays that exist in a beam, or pencil, at an angle β from the axis and whose energy is between E_1 and

$E_1 + \Delta E_1$. For small ΔE_1 (small meaning that for any E_1' in the range ΔE_1, $\tau(E_1)$ and $\tau(E_1 + \Delta E_1)$ are different from $\tau(E_1')$ by not more than some number whose magnitude will be discussed later), the number of pulses, $C(\beta, E_1)$, recorded in a given time due only to gamma-rays within ΔE_1 and within the pencil at angle β is approximately proportional to the term

$$(1 - e^{-\tau(E_1)x(\beta)})$$

of the integral $J_n(E_1)$. With an experimentally obtained pencil and energy selecting device, then, one is able to find a number proportional to $J_n(E_1)$ by recording the number of pulses for a given time t_1 at several values of β between zero and γ, and either numerically or graphically integrating the result; that is, equation (4) becomes

$$J_n(E_1) = K \int_0^{\gamma} C(\beta_i E_1)\, P_n(\cos\beta_i)\, \sin\beta_i\, d\beta_i \qquad (5)$$

where $C(\beta_i, E_1)$ is the number of pulses recorded in t_1 and K is a quantity in part dependent on t_1. The desired ratio then becomes

$$\frac{J_n(E_1)}{J_o(E_1)} = \frac{\int_0^{\gamma} C(\beta_i, E_1)\, P_n(\cos\beta_i)\, \sin\beta_i\, d\beta_i}{\int_0^{\gamma} C(\beta_i, E_1)\, \sin\beta_i\, d\beta_i} . \qquad (6)$$

This indicates that an experiment can be designed to determine the Q_n at any energy which will give a result

that can be compared with the theoretically calculated values.

The integrals J_n/J_o(n = 2,4) have been calculated (3, p. 719) from the form of J_n given in equation (4) using theoretical values of τ. These calculations were specifically for a 1.5 inch diameter cylindrical NaI(Tl) crystal for several source distances, crystal heights, and gamma-rays of various energies ranging from 0.05 to 5 Mev. Some of these calculations are shown in Figure 5. These calculated ratios were tested experimentally (1, p. 43) over a limited range from the form of J_n given in equation (5). The present experiment has as its purpose the experimental evaluation of the ratios J_n/J_o over an extended range.

EXPERIMENTAL ARRANGEMENT

A pencil of gamma-rays was obtained (as indicated on Figure 2) by mounting a lead brick of suitable dimension in front of a radioactive source. The brick had a cylindrical cavity of approximately one millimeter diameter penetrating it and was mounted so that it could rotate about an axis perpendicular to and going through both the axis of the cavity and the crystal. The point of intersection of these three axes was then the apex of the angle ß. The distance from that point to the center of the crystal face is called the source distance h. The actual source was placed approximately 15 centimeters behind that point to provide a well collimated pencil.

The voltage pulse output of the photomultiplier underwent two stages of linear amplification, the linearity being desirable in that the pulse height would be proportional to the gamma-ray energy for ease of energy selection.

Energy selection was accomplished with a pulse height analyzer after the pulse amplification stage. J_n/J_o was determined at three source distances h (h=5,7,10 centimeters) for five different energies ranging from 0.1 Mev. to 0.8 Mev. It was previously mentioned that the term $(1 - e^{-\tau(E_1)x(\beta)})$ calls for the absorption coefficient at a particular energy, say E_1, whereas experimentally the

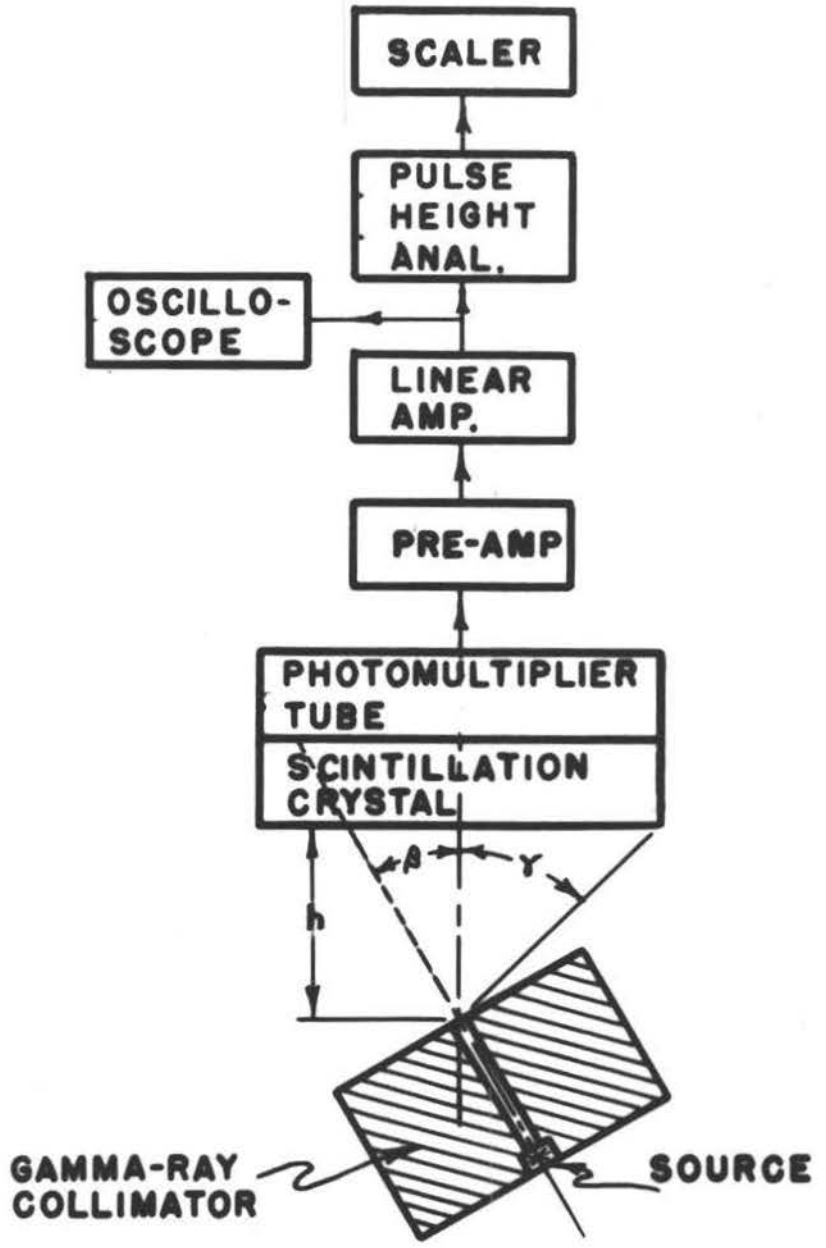

Figure 2. Block diagram of the experimental apparatus.

total counts accepted by the analyzer due to gamma-rays in the energy range ΔE_1 were used which therefore introduces an experimental error which decreases with decreasing ΔE_1 and of course is small at any circumstance provided $\partial \mathcal{C} / \partial E$ is small in the energy region ΔE_1. The actual extent ΔE_n of the energy spectrum of a gamma-ray with nominal energy E_n accepted by the analyzer is indicated on the energy distribution curve for a typical source by the vertical lines AA on Figure 4. The decision to bracket a complete energy peak was a compromise due to several factors. It would seem desirable to choose a smaller ΔE_n such as is indicated by the vertical lines BB on Figure 4, but under such conditions a small shift of the energy peak relative to the bracketing lines will change the counting rate for reasons not of interest in this experiment; i.e. a new undesirable variable becomes prominent. It was found that the energy peak shifting relative to the minimum and maximum energy settings of the pulse height analyzer was significant and warranted choosing both settings such that the vertical lines were in regions of energy where the counting rate was nearly constant thus minimizing the effect of this objectionable variable. Another alternative was to set the lines at the top of the peak (lines CC Figure 4) where the counting rate approaches constancy but in doing so, the

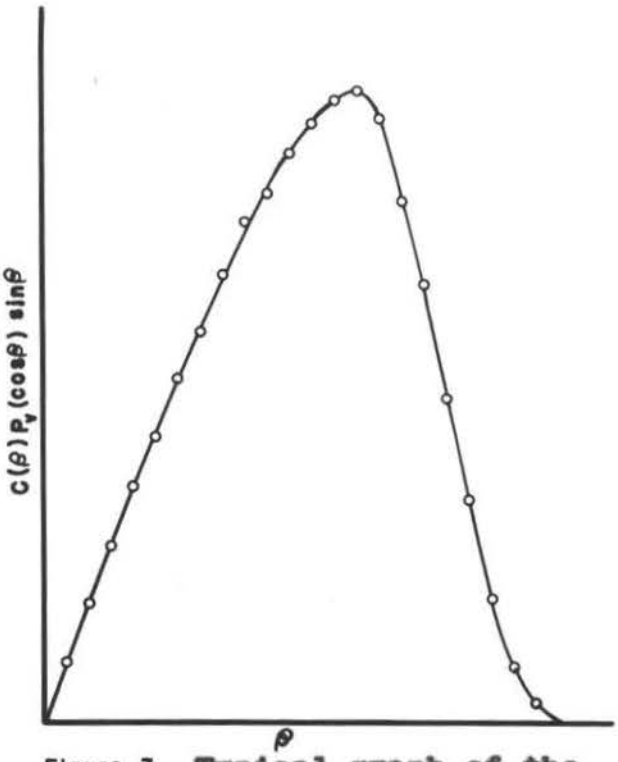

Figure 3. **Typical graph of the integrand of J_n versus angle β**

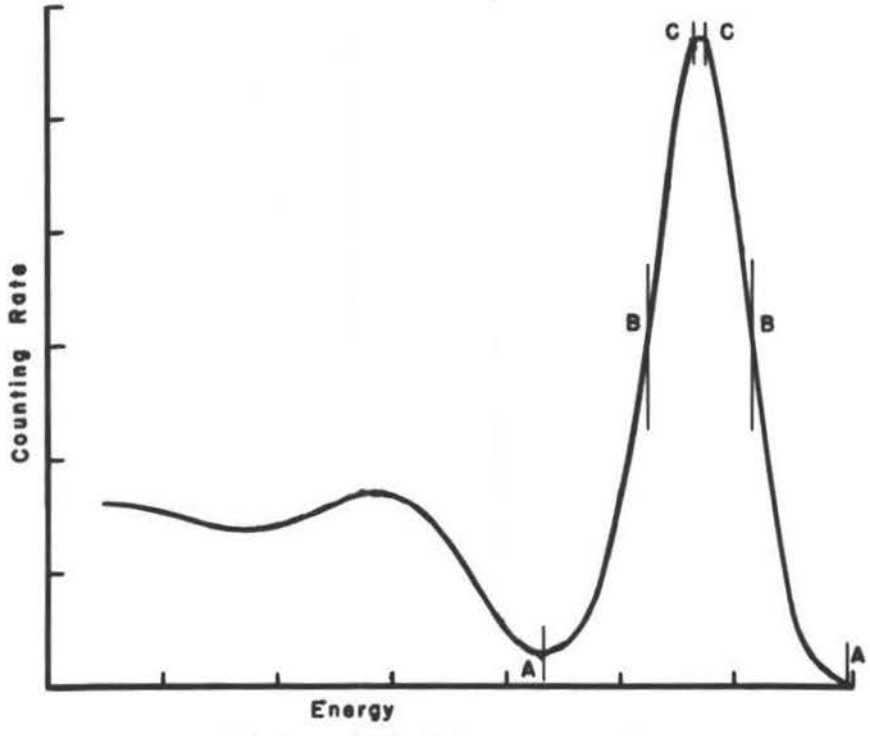

Figure 4. **Pulse height spectrum**

counting rate for a given source strength is reduced many-fold, thus increasing the time necessary to perform the experiment for a fixed experimental accuracy. Upon choosing the total energy peak as ΔE_n, the problem of drifting was not fully eliminated but was kept under surveillance while taking data, for example, by periodically setting the energy range minimum to a standard point E_s on the spectrum where $\partial C/\partial E << -1$ and the energy range maximum to a value such that all detected photons of energy greater than E_s were recorded. Then only if the counting rate remained constant within the statistical fluctuation was the data accepted.

Coupled to the output of the linear amplifier was an oscilloscope which insured against overdriving the linear amplifier and thereby getting nonlinear amplification.

Five different sources were used to obtain five energy peaks. Each is listed below with its corresponding energy and half-life.

Table I

Source	Energy of peak in Mev	Half-life
Ce^{141}	0.14	33 days
Hg^{203}	0.28	47 days
Sn^{113}	0.39	119 days
Cu^{64}	0.51	12.8 hours
Zr^{95}	0.75	65 days

Only for Cu^{64} was the half-life of such duration that correction for decay was made before calculating J_n.

The source strengths varied over a range from 1 to 10 millicuries. For some the counting rate was of sufficient magnitude that corrections for dead time of the system were necessary.

Q_n were determined for different scintillation crystals of the same nominal specifications in identical geometries and no important differences were observed.

The J_n were calculated by graphically integrating the plot of $C(\beta_i)\ P_n(\cos\beta_i)\ \sin\beta_i$ as a function of β_i typically illustrated in Figure 3 where $C(\beta_i)$ is the counting rate (corrected for background) recorded with the gamma-ray beam at angle β_i. For all energies and source distances considered, the J_n were calculated twice using independent data; that is, upon recording the counting rate from $\beta_i = 0$ through $\beta_i = \gamma$, the crystal was rotated about its axis through some angle and $C(\beta_i)$ recorded again, and J_n was calculated from each set of data. The final evaluation of J_n/J_o taken was the average of the two determinations.

RESULTS

The experimental results are listed in Table II below and are compared graphically with the Stanford and Rivers (3, p. 719) calculations in Figure 5.

TABLE II

Energy (Mev)	J_2/J_o			J_4/J_o		
h in centi-meters	5	7	10	5	7	10
0.14	0.9095	0.9475	0.9791	0.7283	0.8396	0.9177
0.28	0.9217	0.9540	0.9777	0.7606	0.8579	0.9242
0.39	0.9308	0.9560	0.9814	0.7760	0.8654	0.9339
0.51	0.9258	0.9550	0.9829	0.7765	0.8630	0.9313
0.75*	0.9305	0.9559	0.9815	0.7790	0.8684	0.9247

*(0.75 Mev is the approximate mean of three peaks unresolvable with the apparatus used.)

The agreement between the experimental results and the calculations appear to be sufficiently good in spite of the fact that the detecting device accepted a range of gamma-ray energies so that the attenuation coefficients of Stanford and Rivers can be used with scintillation detectors of cylindrical geometry over the approximate extended range of energies from 0.10 Mev to 3.00 Mev.

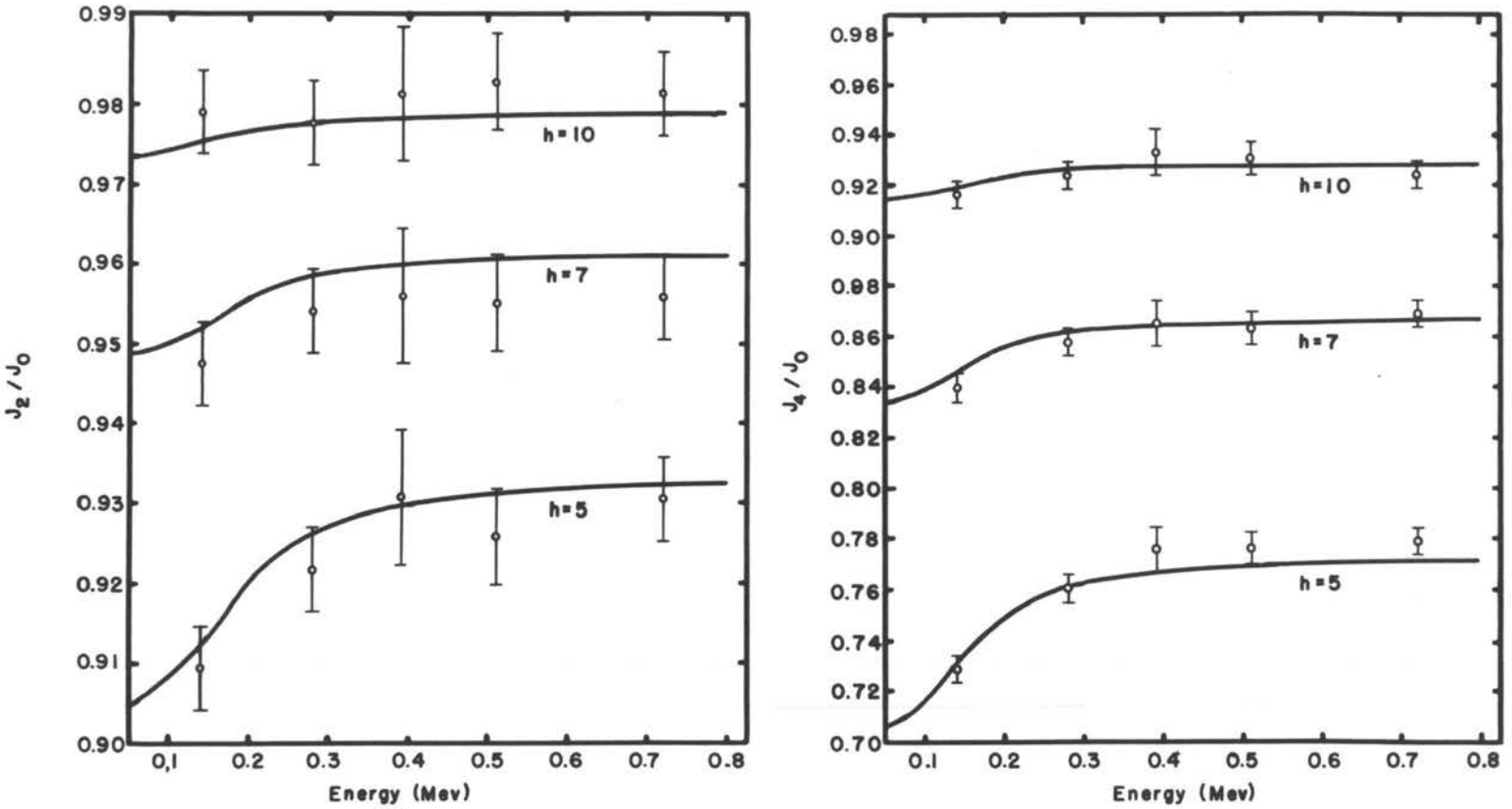

Figure 5. Attenuation factors versus energy

BIBLIOGRAPHY

1. Glasgow, Dale W. Gamma-gamma directional correlation in magnesium-24. Ph.D. thesis. Corvallis, Oregon State University, 1961. 76 numb. leaves.

2. Margenau, Henry and George M. Murphy. The mathematics of physics and chemistry. New York, D. Van Nostrand Company Inc., 1961. 109p.

3. Stanford, A. L., Jr. and W. K. Rivers. Angular correlation and angular distribution attenuation coefficients. The Review of Scientific Instruments 30:719-721. 1959.

4. Rose, M. E. The analysis of angular correlation and angular distribution data. The Physical Review 91:610-615. 1953.

APPENDIX

UNCERTAINTY CALCULATIONS

The ratios J_n/J_o, as indicated above, are the average of two calculations, here distinguished by the second subscripts so that

$$J_n/J_o = 1/2\ (J_{n1}/J_{o1} + J_{n2}/J_{o2}).$$

The uncertainty in this quantity is

$$\Delta(J_n/J_o) = 1/2 \left(\left[\Delta(J_{n1}/J_{o1})\right]^2 + \left[\Delta(J_{n2}/J_{o2})\right]^2 \right)^{\frac{1}{2}}$$

where

$$\Delta(J_{n1}/J_{o1}) = J_{n1}/J_{o1} \left((\Delta J_{n1}/J_{n1})^2 + (\Delta J_{o1}/J_{o1})^2 \right)^{\frac{1}{2}}$$

and similarly for $\Delta(J_{n2}/J_{o2})$. Approximations such as

$$\Delta J_{n1}/J_{n1} = \Delta J_{o1}/J_{o1} = \Delta J_{o1}/J_{n1} = \Delta J_{o2}/J_{o2}$$

simplify the uncertainty to

$$\Delta(J_n/J_o) = \Delta J_{o1}/J_{o1}$$

where J_{o1} is the area under the curve typified in Figure 3 and ΔJ_{o1} is the uncertainty of the area. The uncertainty causes considered were

1) uncertainty in the recorded counting rate due to statistical fluctuation,
2) inability to visually fit the best curve to the points, and
3) errors of graphical integration.

Let c_i be the total number of pulses counted at angle β_i and B the background count so that the ordinate

plotted in Figure 3 is

$$N_i = (c_i - B)\, P_n (\cos \beta_i) \sin\beta_i .$$

With the uncertainty in β_i as zero, the uncertainty in N_i is

$$\Delta N_i = \sqrt{(\Delta c_i)^2 + (\Delta B)^2}$$

where Δc_i and ΔB are the uncertainties of c_i and B. Since the gamma-ray emissions are random these uncertainties equal the square root of the total count so that

$$\Delta N_i = \sqrt{c_i + B} \ .$$

ΔJ_o was then evaluated by graphing both N_i and $N_i + \Delta N_i$ as a function of β_i and finding the difference in their graphical integration. Except for energies 0.39 Mev and 0.51 Mev, $\Delta(J_n/J_o)$ was negligible in comparison to uncertainties arising from other causes. The uncertainties found for 0.39 Mev and 0.51 are approximately 0.007 and 0.003 respectively.

Uncertainties due to errors of curve fitting were found relatively negligible.

The largest errors arose in graphical integration but are conveniently all nearly equal since the graphs (Figure 3) were forced to have approximately equal dimensions. The uncertainty, ΔJ_o, was determined by graphically integrating the same curve several times and applying the relation

$$\Delta J_o = \sqrt{\frac{\sum_{j=1}^{q} (\Delta J_{oj})^2}{q - 1}}$$

This uncertainty is approximately 0.006.

The approximate total uncertainties are listed in Table III below and included in Figure 5.

TABLE III

Uncertainties of J_n/J_o

Energy (Mev)	ΔJ_o
0.14	0.006
0.28	0.006
0.39	0.009
0.51	0.007
0.75	0.006